

Supporting information for

In-situ Growth of Biocidal AgCl Crystals in the Top Layer of Asymmetric Polytriazole Membranes.

*Luis Francisco Villalobos,^a Stefan Chisca,^b Hong Cheng,^c Pei-Ying Hong,^c Suzana Pereira Nunes,^b and Klaus-Viktor Peinemann^{*a}*

^a Advanced Membranes and Porous Materials Center, King Abdullah University of Science and Technology (KAUST), Kingdom of Saudi Arabia

^b Biological and Environmental Science and Engineering Division (KAUST), Kingdom of Saudi Arabia

^c Water Desalination & Reuse Center, King Abdullah University of Science and Technology (KAUST), Kingdom of Saudi Arabia

*E-mail: klausviktor.peinemann@kaust.edu.sa

Outline

1, Polytriazole (PTA) characterization

2, Effect of second bath (non-solvent bath)

2.1, Tap water versus Milli-Q water

2.1.1, Size distribution of AgCl crystals

2.1.2, XPS

2.1.3, XRD

2.1.4, Membranes' performance (permeance and MWCO)

2.1.5, Antimicrobial character

2.2, Aqueous NaBH₄ solution

3, References

1, Polytriazole (PTA) characterization

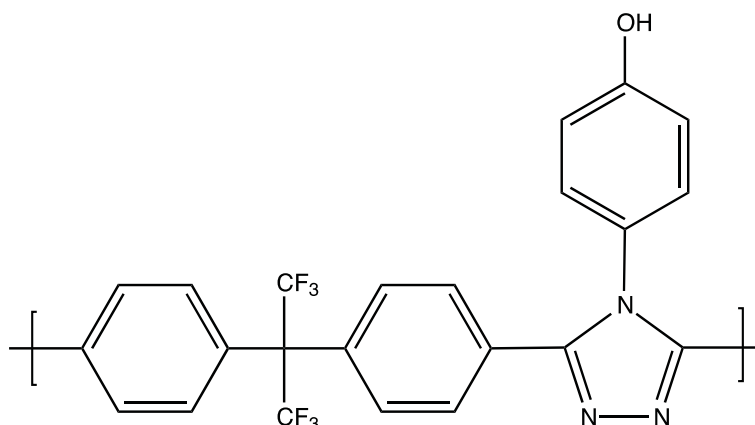


Figure S1. Structure of polytriazole (PTA).

The structure of polytriazole is depicted in Figure S1. It was investigated by FTIR (Figure S2). The conversion of oxadiazole rings into triazole rings is confirmed by the presence of a new intense peak at 1514 cm^{-1} , which is characteristic for triazole,¹ while the characteristic peaks for oxadiazole, at 1070 and 1018 cm^{-1} , almost disappear.^{2,3} The presence of grafted OH groups is proved by the presence of the broad peak in the range $3000 - 3500\text{ cm}^{-1}$. The sharp peak at 1496 cm^{-1} in the polyoxadiazole spectrum is characteristic for $\text{C} = \text{C}$ linkages of aromatic rings,⁴ while in the polytriazole spectrum this peak is shifted to 1476 cm^{-1} and is more broad, due to overlap with the triazole peak.

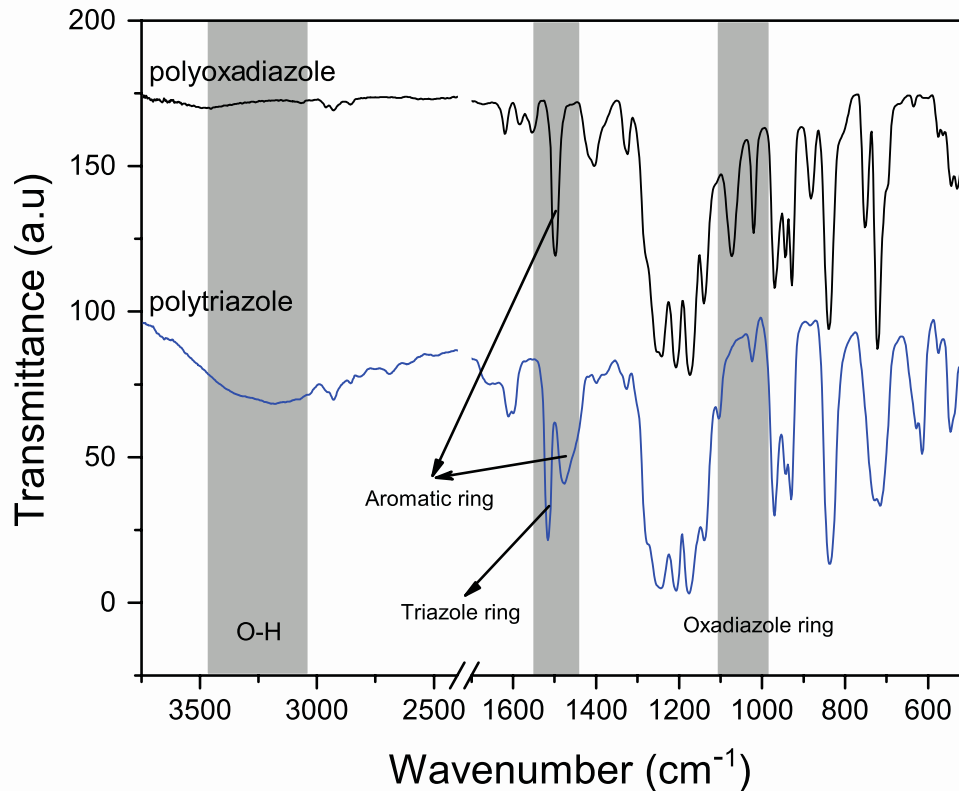


Figure S2. FTIR spectra of polyoxadiazole precursor and polytriazole.

2, Effect of second bath (non-solvent bath)

The silver-triazole complexes formed in the first bath are not stable in water. The silver leaches out from the membrane when it is immersed in a water bath. There are other options of non-solvents for the second bath (e.g. isopropanol, ethanol, etc.) that can also precipitate a porous support. However, using something else besides water for the second bath increases the manufacturing costs and complexity. Besides the membranes will eventually contact a water stream during operation. To avoid silver ions to escape in contact with the non-solvent water bath we decided to try two strategies: fix them in either silver nanoparticles (AgNPs) or AgCl crystals reservoirs. Using of tap water containing Cl^- ions as the non-solvent bath will precipitate AgCl crystals in the top layer of the membrane. Moreover, using an aqueous solution of sodium borohydride (NaBH_4) will form AgNPs in the top layer of the membrane.

2.1, Tap water versus Milli-Q water

The tap water available in our laboratory comes directly from an in-house reverse osmosis plant located on the shore of the Red Sea and contains an average concentration of chloride ions of 63.5 mg/L. It can be observed in the SEM and TEM images presented in Figure 3 that the membranes prepared with tap water contain AgCl crystals on their surface and in the selective layer's polymer matrix. XPS and XRD data on membrane's surface further corroborates this. Membranes prepared by tap water contained the same atomic wt.% of Cl and Ag in their surface while membranes prepared using Milli-Q water contain no Cl (Figure S4). Moreover, the surface of a membrane prepared with tap water shows clear diffraction peaks that matches AgCl's crystal lattice characteristic peaks while membranes prepared using Milli-Q water lack these diffraction peaks (Figure S5).

2.1.1, Size distribution of AgCl crystals

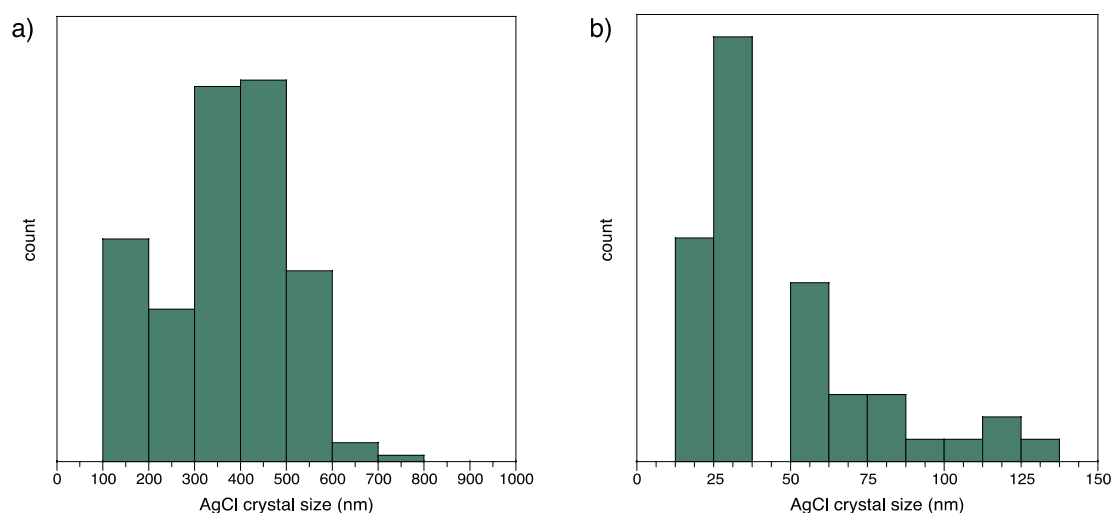


Figure S3. Size distribution histograms of AgCl crystals on the surface (a) and inside the top selective layer (b) of PTA/Ag(100,tap) membrane.

2.1.2, XPS

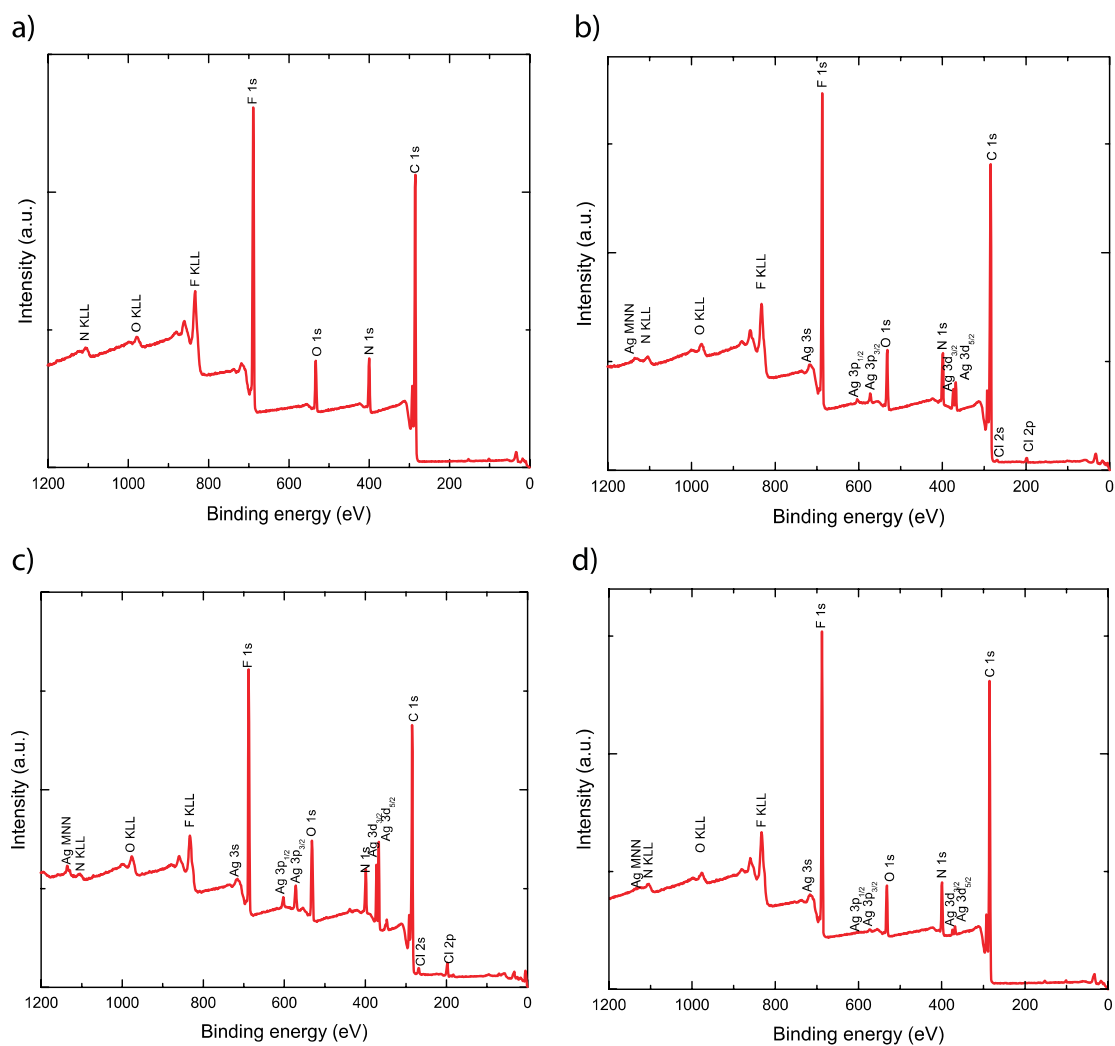


Figure S4. XPS spectra of the surface of: a) blank PTA membrane, b) PTA/Ag(100,tap), c) PTA/Ag(500,tap), and d) PTA/Ag(500,Milli-Q).

2.1.3, XRD

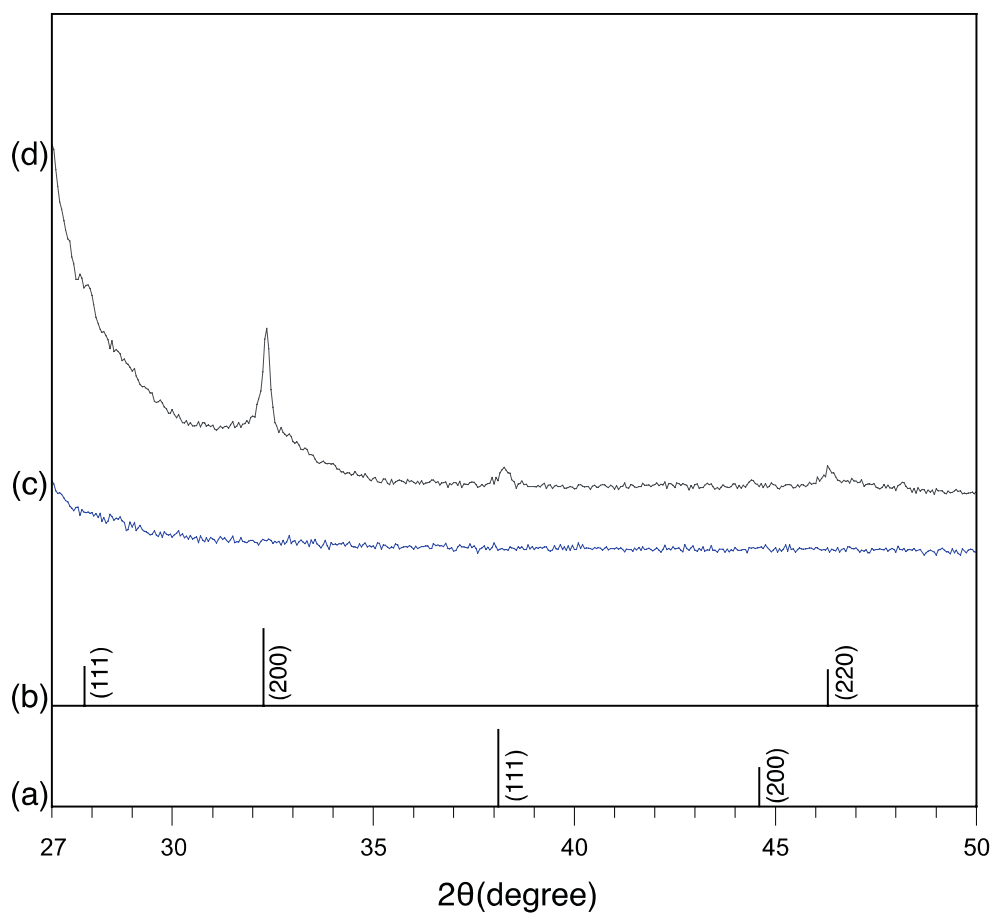


Figure S5. a) X-ray diffraction pattern of: a) Ag^0 (JCPDS 65-2871), b) AgCl (JCPDS 31-1238), c) surface of PTA/Ag(100, Milli-Q), d) surface of PTA/Ag(100, tap).

2.1.4, Membranes' performance (permeance and MWCO)

Figure 2 of the manuscript summarizes the characteristic of PTA/Ag membranes fabricated using tap water. Characteristics of membranes prepared with Milli-Q water instead are summarized in Figure S6.

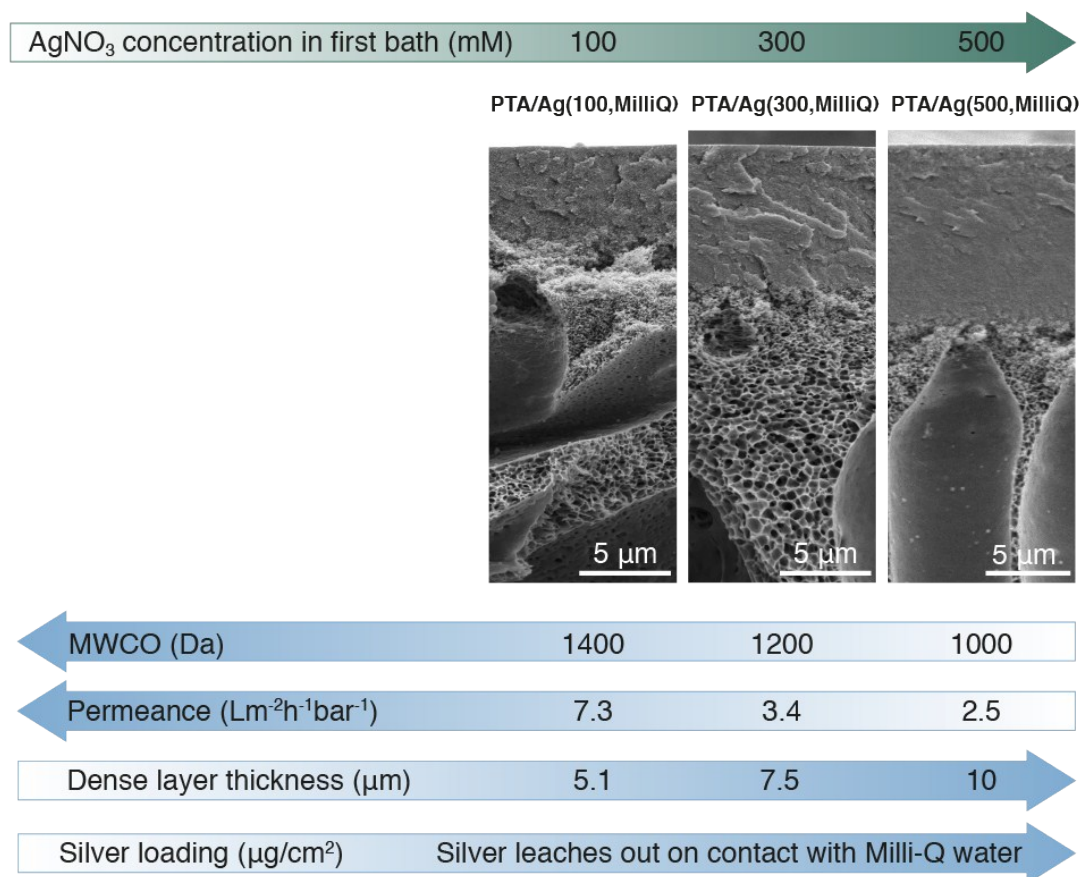


Figure S6. Characteristics and performance of PTA/Ag membranes fabricated with different AgNO₃ concentrations in the first bath and using Milli-Q water for the second bath.

2.1.5, Antimicrobial character

Figure 3a of the manuscript shows the antimicrobial character of PTA/Ag membranes fabricated using tap water. The results for membranes prepared with Milli-Q water instead are summarized in Figure S7. Their antimicrobial character is much lower than their AgCl-containing counterparts.

Figure S8 depicts the surface of three different membranes imaged by SEM just after the antimicrobial activity test. It can be observed that several bacteria are attached to the blank PTA membrane and to PTA/Ag(100,Milli-Q). Some cells attached to PTA/Ag(100,Milli-Q) exhibit signs of a compromised integrity— appear flattened in the SEM image—indicating some antimicrobial activity. No signs of attached cells could be observed in PTA/Ag(100,tap) membrane indicating a high antimicrobial activity.

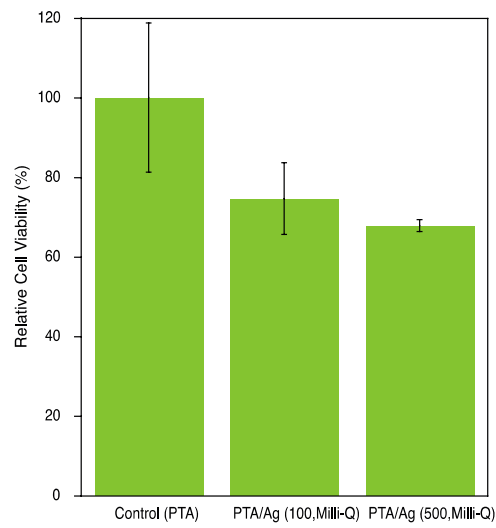


Figure S7. Growth inhibition of suspended bacteria after exposing the membranes to *Pseudomonas aeruginosa* PAO1 for 24 h.

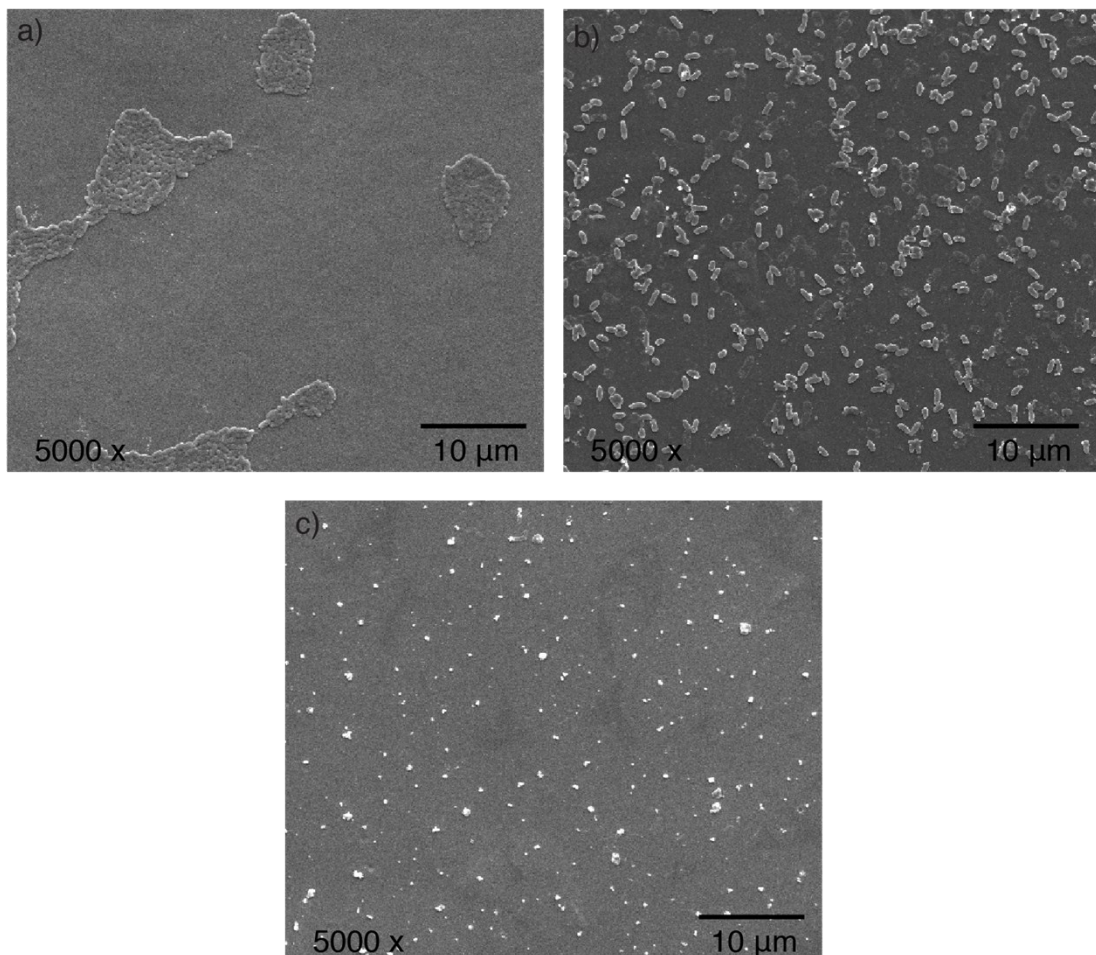


Figure S8. Images of the surface of membranes after exposing them to *Pseudomonas aeruginosa* PAO1 cells for 24 h. a) Blank PTA membrane. b) PTA/Ag(100, Milli-Q). c) PTA/Ag(100, tap).

2.2, Aqueous NaBH₄ solution

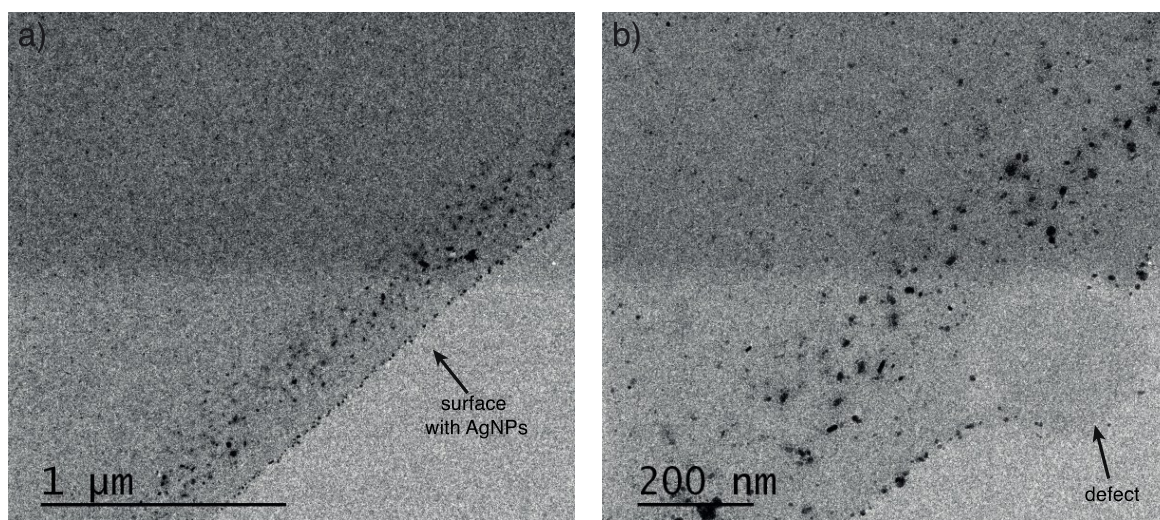


Figure S9. TEM images of a membrane prepared using 100 mM AgNO₃ in the first bath and a 0.05 M NaBH₄ aqueous solution for the second bath.

3, References

- (1) Huang, S.-T.; Liaw, D.-J.; Hsieh, L.-G.; Chang, C.-C.; Leung, M.-K.; Wang, K.-L.; Chen, W.-T.; Lee, K.-R.; Lai, J.-Y.; Chan, L.-H.; Chen, C.-T. Synthesis and electroluminescent properties of polyfluorene-based conjugated polymers containing bipolar groups. *J. Polym. Sci. A Polym. Chem.* **2009**, *47*, (22), 6231-6245.
- (2) Gomes, D.; Marschall, R.; Nunes, S. P.; Wark, M. Development of polyoxadiazole nanocomposites for high temperature polymer electrolyte membrane fuel cells. *J. Membr. Sci.* **2008**, *322*, (2), 406-415.
- (3) Gomes, D.; Nunes, S. P. Fluorinated polyoxadiazole for high-temperature polymer electrolyte membrane fuel cells. *J. Membr. Sci.* **2008**, *321*, (1), 114-122.
- (4) Damaceanu, M.-D.; Constantin, C.-P.; Nicolescu, A.; Bruma, M.; Belomoina, N.; Begunov, R. S. Highly transparent and hydrophobic fluorinated polyimide films with ortho-kink structure. *Eur. Polym. J.* **2014**, *50*, 200-213.